J. Membrane Biol. 132, 27–40 (1993)

The Journal of
Membrane Biology

Hypotonically Induced Changes in the Plasma Membrane of Cultured Mammalian Cells

Vladimir L. Sukhorukov, W. Michael Arnold, and Ulrich Zimmermann
Department of Biotechnology, Biozentrum of the University of Würzburg, Am Hubland, D-W8700 Würzburg, Germany

Summary. Cells from three cell lines were electrorotated in media of osmotic strengths from 330 mOsm to 60 mOsm. From the field-frequency dependence of the rotation speed, the passive electrical properties of the surfaces were deduced. In all cases, the area-specific membrane capacitance (C_m) decreased with osmolality. At 280 mOsm (iso-osmotic), SP2 (mouse myeloma) and G8 (hybridoma) cells had C_m values of 1.01 ± 0.04 μF/cm^2 and 1.09 ± 0.03 μF/cm^2, respectively, whereas dispase-treated L-cells (sarcoma fibroblasts) exhibited C_m = 2.18 ± 0.10 μF/cm^2. As the osmolality was reduced, the C_m reached a well-defined minimum at 150 mOsm (SP2) or 180 mOsm (G8). Further reduction in osmolality gave a 7% increase in C_m, after which a plateau close to 0.80 μF/cm^2 was reached. However, the whole-cell capacities increased about twofold from 200 mOsm to 60 mOsm. L-cells showed very little change in C_m between 280 mOsm and 150 mOsm, but below 150 mOsm the C_m decreased rapidly. The changes in C_m correlate well with the swelling of the cells assessed by means of van't Hoff plots. The apparent membrane conductance (including the effect of surface conductance) decreased with C_m, but then increased again instead of exhibiting a plateau. The rotation speed of the cells increased as the osmolality was lowered, and eventually attained almost the theoretical value. All measurements indicate that hypo-osmotically stressed cells obtain the necessary membrane area by using material from microvilli. However, below about 200 mOsm the whole-cell capacities indicate the progressive incorporation of "extra" membrane into the cell surface.

Key Words membrane stress · osmotic pressure · membrane conductivity · membrane capacity · electrorotation

Introduction

Many wall-less cells are capable of withstanding an osmotic shock by means of large and rapid changes in surface area. This response is of physiological and biotechnological, as well as of biophysical interest. Thus, desert animals must be able to undergo considerable fluctuations in the osmolality of their body fluids without damage. In plants, the changes in area of the plasma membrane that result from cellular dehydration and subsequent rehydration during freezing and thawing may contribute to cell death [39]. Osmotic shock is also useful in the production of hybrid cells via electrofusion (*see below*).

The increase in apparent surface area after a hypo-osmotic shock requires one or more of: (i) a "stretching" of existing planar membrane (but this can only give a few percent area increase, at least in erythrocytes [30]); (ii) the unfolding of nonplanar areas of plasma membrane (such as microvilli [28]); (iii) the almost instantaneous production of "extra" plasma membrane, presumably by reutilization of internal membranes or by mobilization of stored membrane.

In order to distinguish between these mechanisms, measurement of the electrical charging-time of the plasma membrane seems to be a promising approach. The membrane time constant (τ) increases with cell radius, membrane capacity, and with other factors whose importance depends on the suspension medium conductivity [9, 31, 35–37]. In very low conductivity media (30 μS/cm or less) the internal conductivity is usually high enough that it is to be neglected [9, 40], but the membrane conductivity and/or the surface conductance exert significant influence on τ [9, 24, 35]. These parameters can be expected to change in characteristic ways according to how the membrane area increases. Indeed, interesting data on the membrane capacity of hypo-osmotically stressed cell populations have been obtained from impedance spectroscopy [11]. However, the membrane time constant may also be measured by electrorotation [2–10, 18–22, 32, 35–37], which has some advantages here. Thus, measurements of rotation speed can also give information on the hydrodynamic resistance of the cell (which should be affected by the presence of membrane folds or villi). In addition, this single-cell method can directly detect changes in the heterogeneity of the population (which are expected in response to stress).

Electrorotational investigation of cellular osmotic response has been carried out on an insect ova cell line [17]. The recent finding that production of

hybridoma cells by electrofusion is enhanced when the fusion is carried out after a severe hypo-osmotic shock [1, 16, 27, 34, 41] encouraged this study of myeloma and hybridoma cells. These are suspension-cultured cells; work on surface-dependent cells (fibroblasts) is included for comparison. Some preliminary results of this work have been presented elsewhere [4].

Materials and Methods

Cells

We used the murine myeloma (nonsecreting) cell line SP2/0-Ag14 [38], the murine hybridoma cell line G8, and L-cells (murine fibroblasts [15]). The G8 line is itself a product of the fusion [34] of splenic B lymphocytes (from C57B1/6 mice) to SP2/0-Ag14 cells. SP2 and G8 cells were cultured in RPMI 1640 medium at 37°C under 5% CO_2 (for details, *see* [41]). Every 2–3 days, the cell suspensions were diluted 1 : 10 with growth medium, in order to keep the cells in the log phase. Measurements were made on cells one day after such a 1 : 10 "split."

L-cells were cultured under conditions similar to those of SP2 and G8 cells. They were detached from the culture flask with 0.01% dispase (Boehringer Mannheim, No. 241750) in RPMI without phenol red (37°C for 1 hr). In order to remove the enzyme, the cells were subjected to three wash cycles (centrifugation at 150 × *g* and removal of the supernatant) with RPMI.

Preparation of Cells for Rotation

Before use, all cells were washed 2–3 times with inositol (Serva, No. I-5125) solutions of the required osmolality (60 to 330 mOsm). The conductivity of the inositol solutions did not exceed 5 μS/cm. In the case of L-cells, inositol solutions contained 0.5 mg/ml of BSA (bovine serum albumin, Serva, No. 11924); 0.2 M HEPES-KOH (Serva, No. 25245, pH 7.4) was used to adjust the conductivity to that desired. Conductivity and osmolality of the solutions were measured by means of a digital conductometer (Knick, GmbH, Berlin) and a cryoscopic osmometer (Osmomat 030, Gonotec GmbH, Berlin), respectively.

Electrorotation Apparatus

The rotation chamber [10] is open at the top for rapid sample replacement, and requires an inverted microscope and (for optimum resolution) a 100× oil-immersion objective. Cell radii were determined with a calibrated ocular micrometer. One filling of the chamber (10 μl) allowed measurement of 3–6 cells.

The determination of the apparent membrane conductivity (G_A) and capacity (C_m) requires measurements at different external conductivities (about 10, 20, 30 or 40 μS/cm), which can be assumed to be negligible compared to the cells' inner conductivity. Since the field is inhomogeneous in the neighborhood of other cells or of the electrodes, only lone cells near the center of the chamber were measured. Conductivity within the chamber was monitored between measurements by the automatic connection of a conductometer to two opposite electrodes.

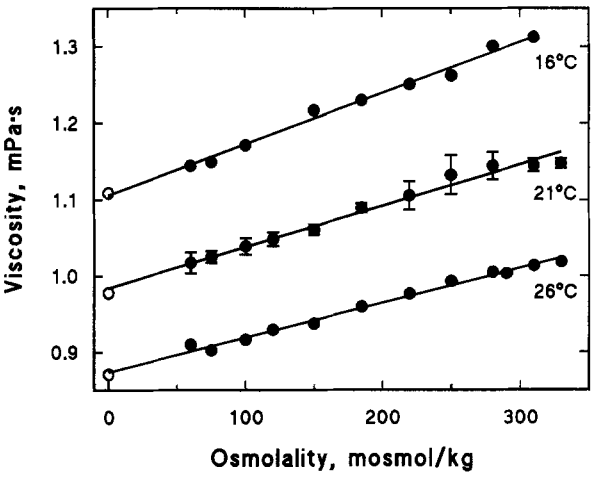

Fig. 1. Dependence of the solution viscosity on the osmolality of inositol solutions at different temperatures. Each point (filled circles) represents the mean value from at least three measurements. The values for water (open circles) were obtained from Ref. [14] and were used to calibrate the apparatus. The data provide good fits to linear functions (solid lines).

The measurements of the field frequency inducing fastest cell rotation (f_C) were performed by the contra-rotating fields technique [2, 8–10], which permits accurate and rapid f_C determination.

In some cases, measurements of the rotation speed at the f_C were also carried out. After determination of the f_C, a single continuous field was applied, and 10 revolutions of the cell were timed with a stopwatch. The field strength of 60 V/cm gave the optimum rotation speed for visual observation. Rotation spectra were stored and evaluated with a videorecorder as before [9]. Measurements were carried out at room temperature (24–26°C).

Viscosity Measurements

In order to allow for the effect of medium viscosity on cell rotation speed, measurements of the viscosity of inositol solutions were performed by means of a falling-ball viscosimeter (HAAKE GmbH, Berlin) at three temperatures (16, 21 and 26°C). Literature values [14] for the viscosity and density of water were used for calibrating the apparatus. The dependence of the viscosity of inositol solutions on their osmolality is shown in Fig. 1.

Rotation Theory

Electrical Parameters of Cells and Media

The electrical properties of isotropic media are well described by the conductivity σ (typical unit: μS/cm) and the absolute permittivity ε (F/cm). On the other hand, the properties of effectively two-dimensional structures such as membranes (subscript "*m*") can helpfully be quoted as *area-specific quantities*: membrane conductivity G_m (mS/cm²) and membrane capacity C_m (μF/cm²), *see* Eq. (2) and Eq. (10). In contrast to σ_m and ε_m, values

for G_m and C_m can be derived without accurate knowledge of the membrane thickness.

A further parameter that is useful when considering microscopic objects in dilute aqueous media is the surface conductance K_S (nS or μS). K_S describes the conductance of an ideally thin surface layer of conductivity σ_S and thickness d:

$$K_S \overset{\lim}{=}_{d\to 0} d \cdot \sigma_S. \tag{1}$$

The significance of a thin layer is that it has no effect on radial charge transport, only on tangential. Layers which contain increased amounts of mobile ions (such as the ionic double layer, the glycocalix, and some cell walls) can be reasonably approximated to surface conductances as long as their thickness does not exceed 10% of the particle radius [A.H. Jäger, W.M. Arnold, and U. Zimmermann, *in preparation*]. The effect of this tangential conductance is to add to the radial, transmembrane conductivity (for diagrammatic representation *see* [24]) to an extent which depends heavily on the radius a. According to [9, 35]:

$$G_A = G_m + (2K_S/a^2). \tag{2}$$

In a weakly conductive medium, the contributions of G_m and of K_S to the G_A of typical cells are expected to be of similar magnitude [35, 36]. They differ only in their dependence on the cell radius, so that separate evaluation of G_m and K_S by means of electrorotation is impossible (unless data from similar cells of various radii are available, *see* [24]). Direct measurement of K_S values is possible when the radial conductivity is negligible. Thus electrorotation could be used to show that the K_S values of polystyrene latex particles are within the range 0.2 to 2.1 nS [6]. On the other hand, determination of G_m alone is possible with very large cells (such as oocytes, $a = 54$ μm, [5]), because the second term in Eq. (2) is negligible when a is large.

At least for initial purposes, the properties of all constituent parts of cells and media are assumed not to change over the frequency range used for rotation (in this work, 4–20 kHz).

The Mechanism of Rotation

A rotating electrical field of a frequency f applied to a suspended cell will generate a rotating dipole within the cell. The interaction of the cell dipole with the rotating field produces a torque and therefore results in rotation. The rotation speed and direction depend on the frequency of the rotating field and on the electrical properties of the medium, cell membrane and cytoplasm [9, 18–22, 33, 36, 37, 40]. Living cells exhibit both anti- and co-field electrorotation, in response to kHz and MHz frequency ranges, respectively. For a cell model consisting of a conductive interior surrounded by a single insulating membrane, with no other sources of dispersion present, the frequency-dependence of the rotation speed (Ω) should be (*see e.g.*, [21]):

$$\Omega = 2A(f/f_c)/(1 + (f/f_c)^2) + 2A_2(f/f_{c2})/(1 + (f/f_{c2})^2) \tag{3}$$

where A, A_2 are the amplitudes, and f_c, f_{c2} the characteristic frequencies of anti-field (A is negative) and co-field (A_2 is positive) rotation, respectively. At the rather low medium conductivities used, the two peaks are widely separated. The co-field peak lies at rather high frequencies and was not measured in this work, because only the anti-field peak yields information on membrane properties.

Typical observed rotation speeds for particles of cell size in aqueous media are a few revolutions per second, and they are determined by the balance between torque and viscous drag. Therefore, the hydrodynamic Reynolds number is not exceeded, and laminar flow is expected. For a Newtonian fluid such as water, the hydrodynamic drag N on a smooth sphere rotating with a speed Ω (radian/sec) is [29]:

$$N = 8 \cdot \pi \cdot a^3 \cdot \eta \cdot \Omega \tag{4}$$

(where a is the cell radius and η is the dynamic viscosity). In the steady state, this can be equated with the electrical torque, so that Ω is predicted to be [6, 9]:

$$\Omega_{(f)} = -U''_{(f)} \cdot \varepsilon \cdot E^2/2\eta \tag{5}$$

where E is the field strength, ε is the absolute permittivity of the medium, and $U''_{(f)}$ represents the frequency-dependent, phase-delayed polarizability of the cell with respect to the medium. ($U''_{(f)}$ is the imaginary part of the Clausius-Mossotti factor, $U^*_{(f)}$ [6, 9], the real part of which determines the dielectrophoretic force [13, 32]). The possible range of speeds is determined by the properties of $U''_{(f)}$: $-0.75 \leq U''_{(f)} \leq 0.75$. As expected from Eq. (3), the peak values of $\Omega_{(f)}$ and of $U''_{(f)}$ are reached in response to the frequency f_c. We use observations of peak Ω and Eq. (5) to calculate experimental peak values (U''_{exp}) of $U''_{(f)}$.

As $U^*_{(f)}$ is a polarizability, it (and therefore $U''_{(f)}$) can also be calculated from the electrical properties of the cell, if these are available. For the kHz-range rotation, which is driven by membrane charging, this theoretical value at the f_c (U''_{the}) is given by (Eq. 37 of [36], modified to include the effect of K_s by substitution of G_A for G_m):

$$U''_{the} = 0.75/(1 + 2\rho_i/\rho_o)[1 + aG_A(\rho_i + 0.5\rho_o)] \tag{6}$$

where $\rho_i = 1/\sigma_i$ and $\rho_o = 1/\sigma_o$ are the internal and external resistivities, respectively, a is the cell radius and G_A is the apparent membrane conductivity (*see* Eq. (2) above). If $\sigma_o \ll \sigma_i$, Eq. (6) becomes:

$$U''_{the} = 1.5/(2 + aG_A/\sigma_o). \tag{7}$$

In this work we compare peak values of U'', derived from the experimental cell speeds measured at the f_c, with those calculated from the f_c-derived electrical parameters. The results enable us to examine the assumption, made in order to use Eq. (4), that we are dealing with a hydrodynamically smooth sphere.

Deviation of Plasma Membrane Parameters from Rotation Data

An ideal, flat, membrane in an electrolyte can be viewed electrically as a parallel-plate capacitor of thickness d and absolute permittivity ε, and capacity (capacitance per unit area) C_{mu}:

$$C_{mu} = \varepsilon/d. \tag{8}$$

This is also a very close approximation for a spherical-shell membrane if $a \gg d$, so that this equation is commonly applied to cell membranes. However, the plasma membrane of many

cells is not smooth: it possesses bulges, folds or microvilli [28]. Therefore, the true membrane area of a cell at physiological osmolality can be much greater than expected from its radius. The *apparent* membrane capacitance C_m (based on the apparent area, $4\pi a^2$) will be increased, say by a factor X:

$$C_m = X \cdot C_{mu} \tag{9}$$

and similarly for G_m. If the membrane irregularities have a radial length that is small compared to the cell radius, then X is also the ratio between true and apparent areas.

The apparent quantities C_m and G_A can be extracted from studying the variation, with medium conductivity (σ_o), of the characteristic frequency of anti-field electrorotation (f_c), because this rotation is due to the charging of the plasma membrane. The theory of single cell electrorotation gives the following relationship between these quantities[1]:

$$f_c \cdot a = \sigma_o/(\pi C_m) + aG_A/(2\pi C_m) \tag{10}$$

This assumes that ($\sigma_m \ll \sigma_o \ll \sigma_i$), where σ_i and σ_m are the intracellular and membrane conductivities, respectively.

The parameters C_m and G_A are extracted by linear regression of $f_C \cdot a$ values against the values of σ_o in which they were measured (*see* Figs. 4 and 5). The regression yields values for the slope (B) and $f_c \cdot a$-intercept (A), which give the required parameters:

$$C_m = 1/\pi B \tag{11}$$

and

$$G_A = 2\pi A C_m/\bar{a} \tag{12}$$

where $\bar{a}$ is the mean radius of the typically 40–80 cells.

Statistics

Results are usually quoted as means and standard errors (SE). Tests of significance between groups of results used Student's t-test, after testing for equal or unequal variance. Most statistics were performed with the program Fig. P, v.6.0 (Biosoft, Cambridge, GB).

Results

Osmotic Swelling

Cells of both suspension cell lines (G8 and SP2) showed a remarkable ability to at least double their apparent surface area (without rupture), in response to hypo-osmotic shock. The radii of those cells measured during the course of electrorotation were assessed.[2]

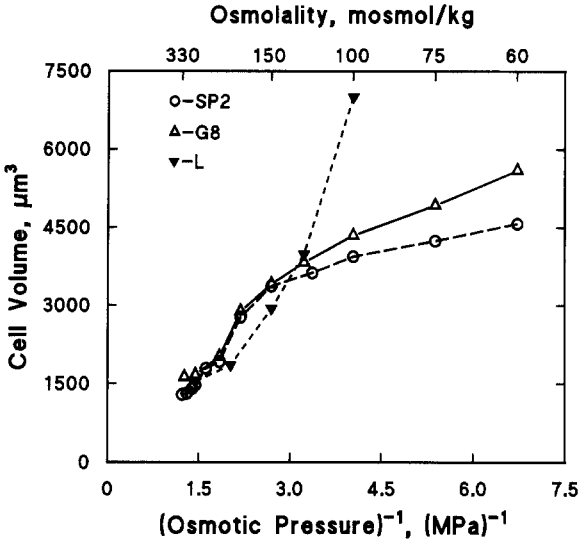

Fig. 2. Dependence of the cell volume of SP2 (○), G8 (△) and L (▼) cells on the reciprocal osmotic pressure ($1/P$). Osmotic pressure was evaluated according to $P = c \cdot R \cdot T$, where c is the osmoticum concentration, R is the gas constant, 8.314 $J \cdot K^{-1} \cdot mol^{-1}$, T is the absolute temperature (298 ± 1 K). Cell volume was calculated from the mean cell radius assuming the cells to be spherical ($V = 4\pi a^3/3$). SP2 and G8 cells show the opposite form of nonlinear dependence on $1/P$ from that of L-cells.

SP2 cell radius was 7.1 ± 0.1 μm (280 mOsm), increasing to 10.3 ± 0.1 μm at 60 mOsm. G8 cells were consistently larger: 7.3 ± 0.1 μm (280 mOsm) and 11.0 ± 0.5 μm (60 mOsm). L-cells (radius 7.2 ± 0.2 μm at 280 mOsm) were not so osmotolerant, and were converted to flaccid "ghosts" by 60 mOsm media. Provided that 0.5 mg/ml BSA was present, 150 mOsm media did not cause this problem. However, the number of apparently turgid, spherical cells decreased to 50% at 100 mOsm (mean radius 11.9 ± 0.4 μm) and to 5–10% at 75 mOsm.

To analyze the swelling behavior, we plotted cell volume (V) against the reciprocal of the medium osmotic pressure (van't Hoff plot). The cell volumes were calculated ($V = 4\pi \cdot a^3/3$) from the radius data. Cells which behave as ideal osmometers should give linear van't Hoff plots, but in all cases they were nonlinear (Fig. 2). Although the initial parts of the plots for SP2 and G8 cells can be approximated to linear functions, we have not shown this in Fig. 2. (The main result of such an

[1] We consider $f_c \cdot a$ instead of f_c because this removes the large influence of the cell radius on the results (the term in $\sigma_o/(\pi C_m)$ usually dominates). This improves the resolution of the method when applied to a size-heterogeneous cell population. The radius of every cell is measured at the same time as its f_c.

[2] These are means ± SEM of the groups of 60–80 cells, as in Figs. 6–8.

exercise, a value for the nonosmotic volume, was found to be critically dependent in magnitude and sign on the number of points included in the regression.) However, the plots do show that the SP2 and G8 cells on the one hand, and the L-cells on the other, exhibit opposite forms of nonlinearity. In highly diluted media, SP2 and G8 cells have smaller volumes, whereas L-cells have larger volumes, than expected from a linear van't Hoff plot. In the isotonic and slightly hypo-osmotic range, L-cells show only a slight dependence of V on reciprocal osmolality. The volume response of L-cells to hypo-osmotic stress is similar to that found for human erythrocytes [30].

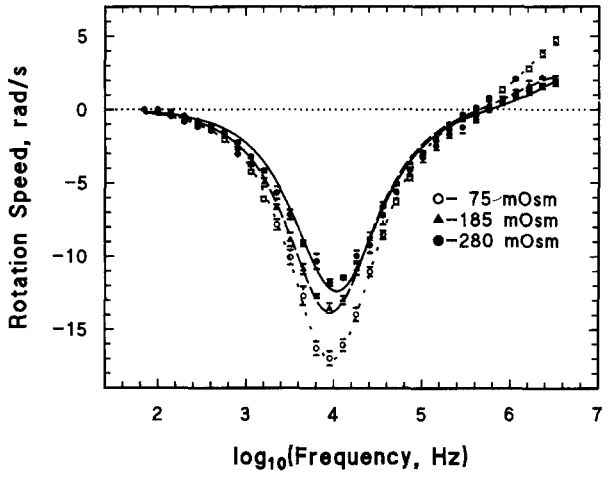

Fig. 3. Rotation spectra of SP2 cells in media of different osmolalities: 280 mOsm (filled circles), 185 mOsm (triangles) and 75 mOsm (open circles), but of the same conductivity (20 ± 1 μS/cm). Each spectrum is the mean obtained from 3–6 cells, the radii of which were (mean ± SE) 10.3 ± 0.3 μm (n = 6), 8.1 ± 0.2 μm (n = 3) and 6.5 ± 0.1 μm (n = 3), respectively. The field frequency was decreased in $\sqrt{2}$:1 steps from 3.277 MHz to 70 Hz at a constant field strength of 90.2 V/cm. The various curves show best fits of Eq. (3) to the experimental points: the Table shows the fitting parameters.

Rotation Spectra

Rotation spectra of SP2 cells at three medium osmolalities are shown in Fig. 3. At the low conductivity used here (σ_o = 20 μS/cm) the fastest anti-field rotation was induced by field frequencies of about 10 kHz. Field frequencies above 1 MHz gave co-field rotation, whose peak was not reached in our experiments. Nevertheless, the size and frequency of this peak (A_2 and f_{c2} in the Table) could be estimated by fitting the data to Eq. (3). Judging by the correlation coefficients, Eq. (3) provides at least a very good approximation to the data.

Dependence of the Anti-Field Peak Frequency on Medium Conductivity

The linear relationship between the $f_c \cdot a$ of anti-field rotation and the medium conductivity (σ_o) predicted by Eq. (10) was observed (Figs. 4 and 5). Experimental data are plotted either as: (Figs. 4*A* and 5*A*) individual $f_c \cdot a$ values, or else (Figs. 4*B* and 5*B*) as mean of $f_c \cdot a$ values from 16–20 $f_c \cdot a$ values measured at closely similar conductivities. This abandons the single cell resolution but provides a better test of linearity of the relationship between $f_c \cdot a$ and σ_o.

In medium of osmolality 60 mOsm, swollen spherical G8 cells (Fig. 4*A*) showed remarkably uniform $f_c \cdot a$ values, so that standard deviations do not exceed 5% of the mean $f_c \cdot a$ values (Fig. 4*B*). Similar results were obtained on SP2 cells (*data not shown*). Neither G8 nor SP2 cells were quite spherical in

Table. The parameters obtained by fitting Eq. (3) to the experimental rotation spectra given in Fig. 3

Osmolality mOsm	Mean f_c (95% confidence limits[b]) kHz	Mean f_{c2}[a] MHz	A rad/sec	A_2[a] rad/sec	r
75	9.52 (9.33–9.72)	4.7 (3.6–6.3)	−17.1	5.1	0.9993
185	9.16 (8.92–9.41)	3.6 (2.4–5.6)	−13.8	2.3	0.9988
280	10.77 (10.14–11.43)	6.5 (0.6–70)	−12.4	2.5	0.9946

[a] "Extrapolated" value: the co-field characteristic frequency f_{c2} was never reached with freshly prepared cells, so that a large uncertainty in the estimate is to be expected. However, it is clear that $f_{c2} \gg f_c$, as required in order to use Eq. (10).

[b] It is appropriate to form the 95% limits on the logarithmic frequency data. Hence, they are not symmetrical about the best estimate, especially when the uncertainty is large.

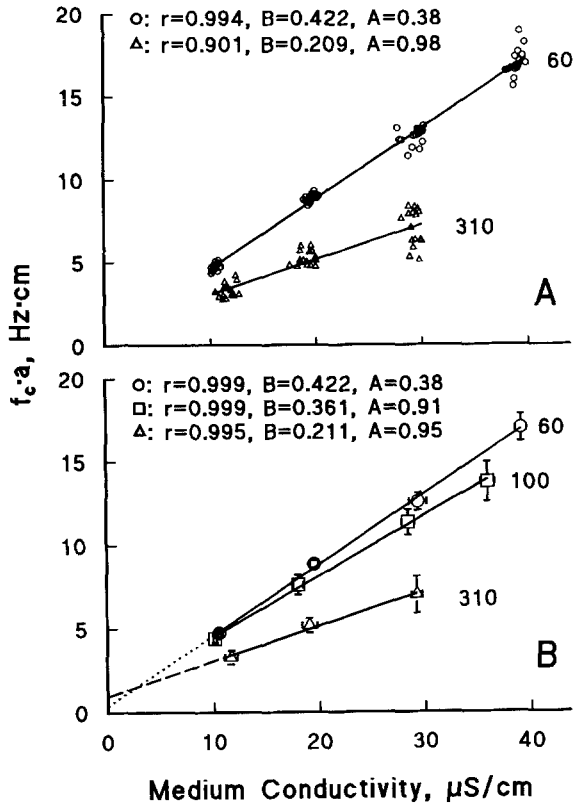

Fig. 4. Primary electrorotation data on G8 cells (SP2 were qualitatively similar) in inositol media of different osmolalities. The frequency of the outer electrical field, which induced the fastest cell rotation (f_c), the cell radius (a) and the medium conductivity were recorded for each cell. The numbers near the lines indicate the medium osmolalities in mOsm. In (*A*), each cell is represented by one symbol, which gives rise to considerable overlapping (48 and 72 cells were measured in this example in media of 310 and 60 mOsm, respectively). Each symbol in (*B*) represents a mean $f_c \cdot a$ value from 16–20 cells measured at closely similar conductivities; standard deviations of the ($f_c \cdot a$) values depicted in the figure did not exceed 12–16% of the means under isotonic conditions and were significantly lower (4–5%) when the measurements were carried out in strongly hypo-osmotic media. The lines plotted in the figure are least-square approximations to the data shown. The slopes and $f_c \cdot a$-intercepts obtained from the mean values in (*B*) were used to calculate the membrane parameters C_m and G_A (Eqs. (10–12)). In all cases the correlation coefficient exceeded 0.995, justifying the use of Eqs. (10–12) for this data.

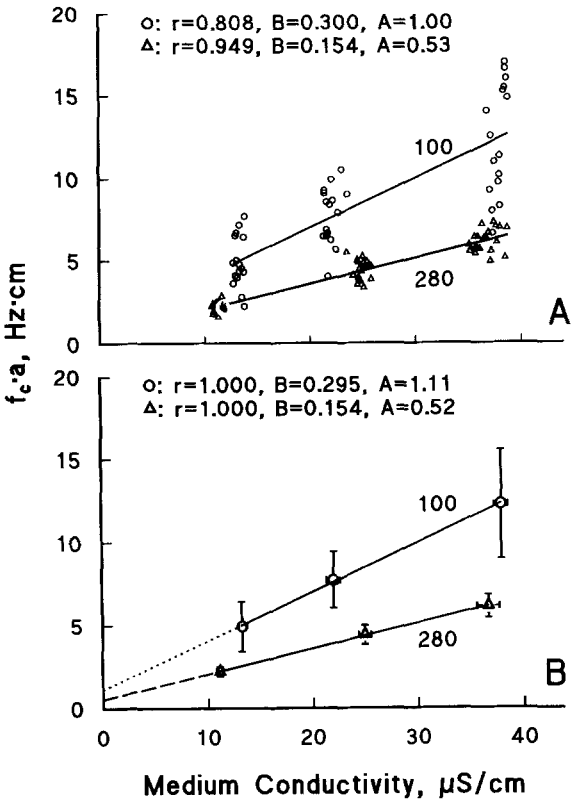

Fig. 5. Primary electrorotation data on L-cells. (For details, *see* legend to Fig. 4). In (*A*), each cell is represented by one symbol (48 cells were measured in each medium, osmolalities 100 and 280 mOsm). Each symbol in (*B*) represents a mean $f_c \cdot a$ value from 16 cells measured at closely similar conductivities. In hypo-osmotic conditions, standard deviations of the ($f_c \cdot a$) values were about 30% of the means, significantly higher than those measured on SP2 or G8 (Fig. 4) cells. Despite this, the mean values show exactly the theoretical and linear dependence on medium conductivity.

media of 250–330 mOsm, and it was more difficult to measure their f_c values than those of hypo-osmotically treated cells. There was also a comparatively large scatter of the $f_c \cdot a$ values (SD about 20%) in these more physiological media.

A completely opposite pattern was seen in the case of L-cells. Standard deviations did not exceed 12% of the mean $f_c \cdot a$ in isotonic media (Fig. 5), but increased to 30% at 100 mOsm. The flaccid "ghost" cells that appeared at 100 mOsm and below (*see above*) did not rotate, indicating that their membranes had been perforated. Despite the scatter of the individual measurements, the mean data from those cells that could be measured at 100 mOsm still showed a highly linear dependence on medium conductivity (Fig. 5*B*). This was not usually the case at 75 mOsm (*no measurements shown*).

C_m and G_A at Different Medium Osmolalities

C_m and G_A were calculated according to Eq. (11) and (12), using the mean $f_c \cdot a$ procedure (as in Figs. 4*B* and 5*B*). At a given medium osmolality the gradients were remarkably reproducible, while the reproducibility of the $f_c \cdot a$-intercept was not as good.

The data so derived for SP2 and G8 cell mem-

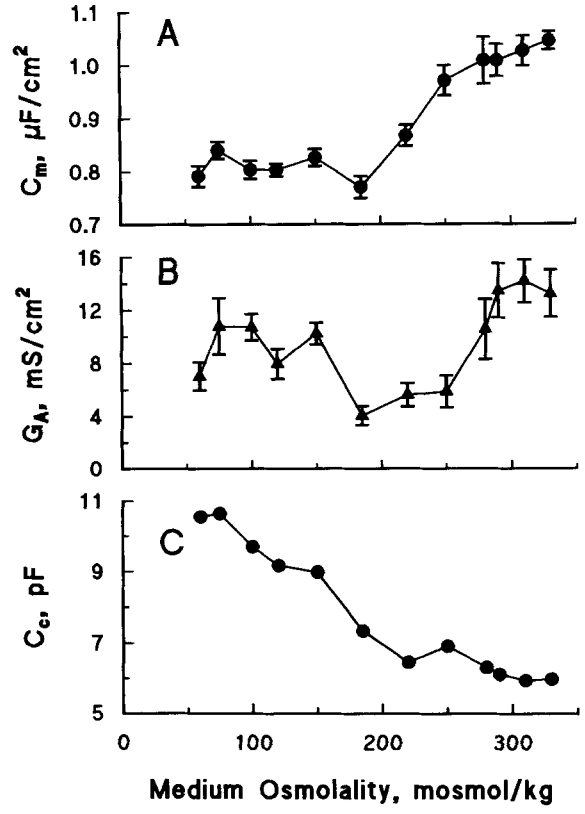

Fig. 6. Dependence of (*A*) the specific membrane capacity (C_m), (*B*) the apparent membrane conductivity (G_A), and (*C*) whole-cell capacitance (C_c) of the SP2 myeloma cells on the osmolality of external medium. The C_c values were calculated from $C_c = 4\pi a^2 \cdot C_m$. The data are the means and standard errors from the following numbers of determinations: 8, 6, 10, 7, 16, 5, 9, 7, 13, 9, 5 and 6 at medium osmolalities 60, 75, 100, 120, 150, 185, 220, 250, 280, 290, 310 and 330 mOsm, respectively. Each determination was as in Figs. 4–5, using at least 48 cells.

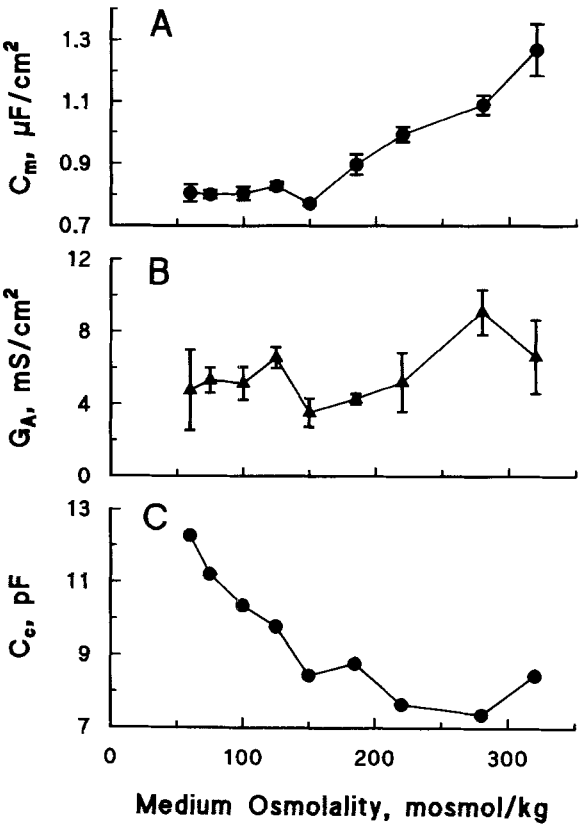

Fig. 7. Dependence of (*A*) the specific membrane capacity (C_m), (*B*) the apparent membrane conductivity (G_A) and (*C*) whole-cell capacitance (C_c) of G8 hybridoma cells on the osmolality of the external medium. The data are the means and standard errors from the following numbers of determinations (as shown in Figs. 4–5): 3, 8, 5, 3, 9, 5, 3, 13 and 4 at medium osmolalities 60, 75, 100, 125, 150, 185, 220, 280 and 320 mOsm, respectively.

branes are shown in Figs. 6*A*, *B* and 7*A*, *B*. Hypo-osmolality induced qualitatively similar alterations to the C_m values in the plasma membranes of these cell lines. For SP2 cells the C_m value decreased at first gradually from 1.05 ± 0.02 μF/cm² (330 mOsm) to 1.01 ± 0.04 μF/cm² (280 mOsm, physiological) and then more rapidly to 0.77 ± 0.02 μF/cm², the minimum value (at 185 mOsm). A small step to 150 mOsm caused a rise to 0.83 ± 0.02 μF/cm² (significantly different from 185 mOsm, $P = 0.077$). Use of more hypotonic media down to 60 mOsm caused little further change.

In the case of G8 cells the C_m decreased rapidly from a rather higher initial value (1.27 ± 0.08 μF/cm² at 320 mOsm) through 1.09 ± 0.03 μF/cm² at the physiological 280 mOsm to a minimum value of 0.77 ± 0.01 μF/cm² at 150 mOsm. As with SP2 cells, the C_m rose slightly on the hypotonic side of the minimum (0.83 ± 0.01 μF/cm² at 125 mOsm, significantly different from C_{m150}, $P < 0.005$), to remain approximately constant (0.80 ± 0.03 μF/cm²) at lower osmolalities (from 125 to 60 mOsm). Measurements at osmolalities higher than 320–330 mOsm were not practical because the cells were not spherical enough for electrorotation measurements.

It is interesting that, for both SP2 and G8 cells, the whole-cell capacitance (C_c, the product of cell area S and C_m):

$$C_c = S \cdot C_m = 4\pi a^2 \cdot C_m \qquad (13)$$

remained almost constant until just before the point of minimum C_m was reached, after which it started to increase.

The dependence of the C_m of L-cells on medium

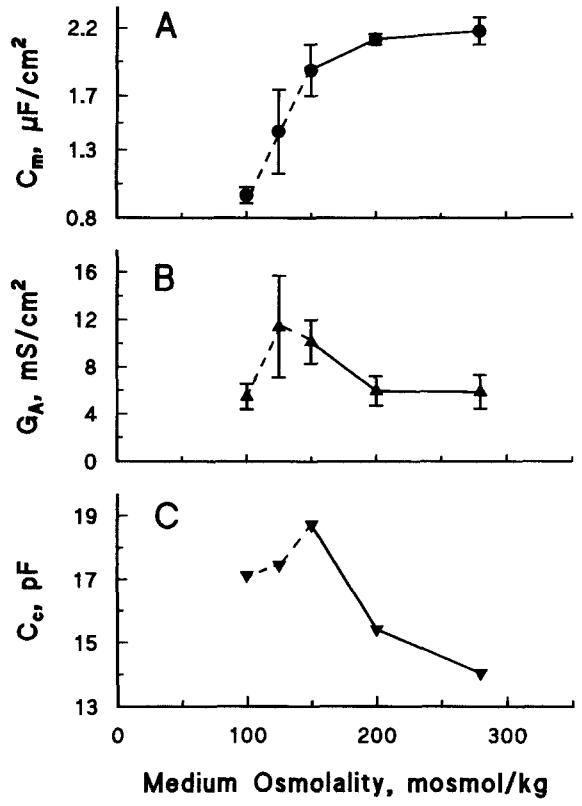

Fig. 8. Dependence of (*A*) the specific membrane capacity (C_m), (*B*) the apparent membrane conductivity (G_A) and (*C*) whole-cell capacitance (C_c) of L-cells on the osmolality of the external medium. The dashed lines indicate that, below 150 mOsm, we may have been dealing with a selected subpopulation of L-cells (*see text*). The data are the means and standard errors from the following numbers of determinations (as in Figs. 4–5): 3, 2, 6, 3 and 5 at medium osmolalities 100, 125, 150, 200 and 280, respectively.

osmolality (Fig. 8*A*) was very different from that of SP2 or G8 cells. Although the value at 280 mOsm (2.18 ± 0.10 μF/cm²) of the fibroblast line was much higher than those of the myeloma and hybridoma lines, decrease of the osmolality had very little effect until about 150 mOsm was reached. Below this osmolality the C_m decreased rapidly. At the lowest osmolality that gave cells of reasonable quality (100 mOsm), the C_m was 0.97 ± 0.06 μF/cm². This does not necessarily mean that the minimum C_m of L-cells is higher than that of SP2 or G8 cells (0.77 μF/cm²) because the scatter between the L-cells at this osmolality is so large (Fig. 5) that the true minimum value will be appreciably lower than the mean value.

As discussed above (*see* Osmotic Swelling), the measurements of L-cells at 125 mOsm and 100 mOsm are of a small percentage of survivors of the osmotic shock. These possibly represent not the average L-cell, but some small (osmo-resistant?) subpopulation. Dashed lines are used to connect these data points in Fig. 8 in order to draw attention to this fact: they do not imply that the measurement technique was unreliable in this region. The decrease of the L-cell C_c values as the osmolality is decreased below 150 mOsm is due, not only to a decrease in C_m, but also to the mean radius not increasing further. This would be consistent with the L-cells only surviving if they do not exceed a critical radius.

The G_A data of SP2 and G8 cells (Figs. 6*B*, 7*B*) exhibit higher scatter than the C_m data. This results from the relatively poor accuracy of G_A determination as well as from day-to-day fluctuations of the cell cultures. Nevertheless, it can be seen that SP2 cells (Fig. 6*B*) show at least three osmolality regions with statistically significant differences in G_A (Fig. 6*B*). Iso- and slightly hyper-osmotic media gave the highest G_A values (10.5–14.2 mS/cm²), but decrease of osmolality to 185 mOsm caused the G_A to decrease to its minimum value (4.1 ± 0.7 mS/cm²). However, further decrease of osmolality (to 150 mOsm and below) caused G_A to return to a much higher range (7.0–10.8 mS/cm²).

The G_A of G8 cells show a similar, but not so pronounced, series of changes as the osmolality is reduced. The maximum value was 9.1 ± 1.2 mS/cm² at 280 mOsm, whereas the minimum was 3.5 ± 0.8 mS/cm² at 150 mOsm. Exactly as with SP2 cells, the minimum G_A occurred at the same osmolality as the minimum C_m.

As with the C_m, the G_A of L-cells responded very differently to that of SP2 or G8 cells. At 280 mOsm the G_A was relatively low (5.8 ± 1.4 mS/cm²), but increased progressively below 200 mOsm to give a maximum at 125 mOsm (11.4 ± 4.3 mS/cm²). The very low apparent value at 100 mOsm (5.5 ± 1.1 mS/cm²) cannot be viewed as representative of the whole population.

Effect of Enzymic Digestion on Cell Membrane Properties

The effect of pronase pretreatment on the membrane electrical properties, cell size and rotation speed of G8 cells is shown in Fig. 9. The cells were treated with the enzyme in isotonic RPMI medium and then transferred into inositol media of osmolalities 75, 150 and 280 mOsm. A statistically significant decrease of the C_m and G_A values after protease treatment was only found in isotonic rotation media (280 mOsm inositol, left pairs of the bar graphs in Fig. 9). The enzyme treatment (n = 4) decreased C_m from 1.05 ± 0.05 to 0.88 ± 0.03 μF/cm² and drastically reduced G_A from 4.3 ± 1.5 to 0.2 ± 0.2 mS/cm². There was a slight increase in mean cell radius from 7.8 ± 0.2 to 8.0 ± 0.2 μm.

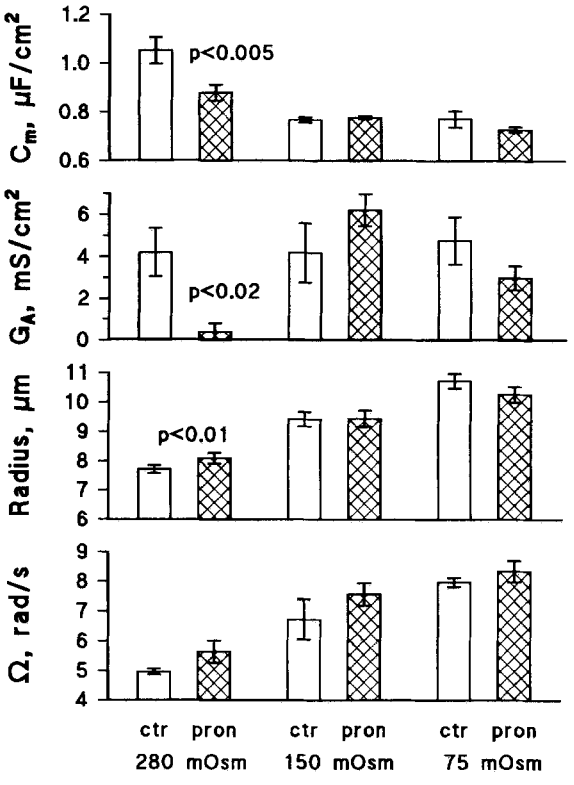

Fig. 9. Effect of pronase digestion on: the passive electrical properties (C_m and G_A), the radius, and on the rotation speed (Ω) measured at the f_c and 60 V/cm, of G8 cells. The enzyme treatment was carried out in isotonic RPMI medium containing 1 mg/ml pronase at 37°C for 10 min. Control cells (bars labeled as *ctr*) were incubated without pronase under the same conditions. After incubation, the cells were washed with low conductivity inositol solution and transferred into inositol media (of 20 μS/cm) of different osmolalities. The pronase treatment caused differences significant at the levels indicated. Where no probability level is shown, the differences were not highly significant ($P > 0.05$).

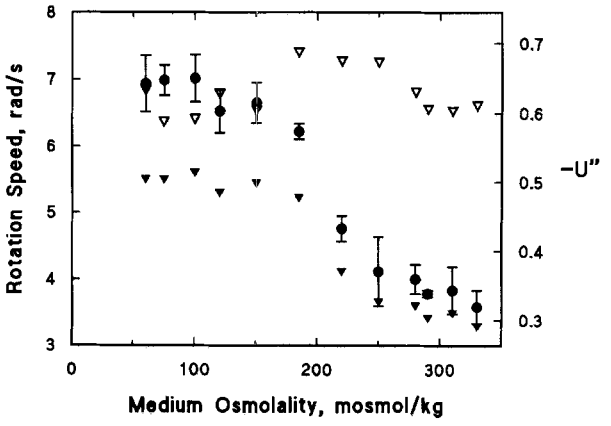

Fig. 10. Interpretation of SP2 cell rotation speeds measured at the f_c. Effect of the medium osmolality on: the peak rotation speed (filled circles); on the experimental peak U''-factor (U''_{exp}, filled triangles) derived from the speed data (Eq. (5), using also the η values from Fig. 1); and on the theoretical peak U''-factor (U''_{the}, open triangles) derived from C_m and G_A values (Eq. (7)). The measurements of the rotation speed were performed by timing of 10 revolutions at individually determined f_c (field strength 60 V/cm). Each rotation speed value (filled circle) represents the mean (with standard error) of data from at least 60 cells.

At lower osmolalities (150 and 75 mOsm) there were no statistically significant differences between control and protease-pretreated cells. However, it is very interesting that the very low G_A of pronase-treated cells at 280 mOsm is increased by hypo-osmotic stress to a similar value to that of untreated cells. These results suggest that membrane alterations induced by protease are insignificant compared to the changes produced by hypo-osmotic stress, and, therefore, that the difference in the behavior of L-cells (from that of G8 or SP2 cells) is not due to the proteolytic step in their preparation.

Comparison of Theoretical and Experimental Rotation Speeds

The rotation speed of SP2 cells, at the optimum field frequency f_c and at a field strength of 60 V/cm, was measured in media of conductivity $\sigma_o = 20$ μS/cm (the open circles in Fig. 10). At high osmolalities the rotation was slow but increased gradually from 3.58 ± 0.25 rad/sec at 330 mOsm to 4.12 ± 0.52 rad/sec at 250 mOsm. Further dilution of the medium caused a rapid increase of the rotation speed from 4.76 ± 0.19 rad/sec at 220 mOsm to 6.23 ± 0.12 rad/sec at 185 mOsm. The fastest rotation (between 6.53 ± 0.33 and 7.02 ± 0.35 rad/sec) was observed between 150 and 60 mOsm. The rotation speed can be assessed as the rotational mobility R ($R = \Omega/E^2$ [22]). The highest value of R was $1.94 \cdot 10^{-3}$ rad · cm² · sec^{-1} · V^{-2}, the lowest was $0.99 \cdot 10^{-3}$ rad · cm² · sec^{-1} · V^{-2}.

A related factor to R, which allows a better comparison between the properties of the *cells* because it compensates for changes in the viscosity and permittivity of the medium, is the peak value of the imaginary part of the Clausius-Mossotti polarizability factor (U'', *see* Eq. (5)). The peak values of U'' are obtained by use of Eq. (5) on the experimental rotation speed data obtained at the f_c (Fig. 10, filled circles) and are therefore termed experimental values (U''_{exp}, the solid triangles in Fig. 10). The dependence of U''_{exp} on the medium osmolality is qualitatively similar to that of the rotation speed (the viscosity changed by only 10–15% over the whole osmolality range studied, *see* Fig. 1; the permittivity of even a 330-mOsm inositol solution is only 1% less than that of water [3]).

We can compare the experimental U''_{exp} with theoretical values, calculated from Eq. (7). The osmolality dependence of U''_{the} (open triangles in Fig. 10) is very different from that of U''_{exp} (filled triangles) or Ω (filled circles).

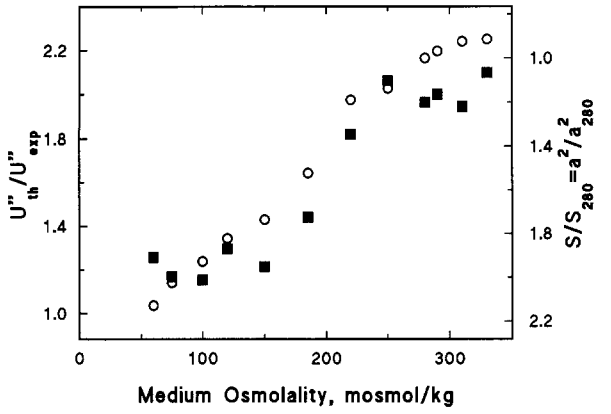

Fig. 11. The ratios U''_{the}/U''_{exp} (filled squares) and S/S_{280} (open circles) at different medium osmolalities. Cell surface area (S) was calculated from $S = 4\pi a^2$ (this assumes an ideal, smooth, spherical surface).

The discrepancy between U''_{the} and U''_{exp} is assessed by the quotient U''_{the}/U''_{exp} (filled squares in Fig. 11). In isotonic media (250–330 mOsm) the discrepancy is large ($U''_{the}/U''_{exp} = 2.1$). Decrease of osmolality gives progressively better agreement between U''_{the} and U''_{exp} until $U''_{the}/U''_{exp} = 1.2$ is attained close to 100 mOsm. It can be seen that the ratio U''_{the}/U''_{exp} is closely correlated with S/S_{280} (open circles), the ratio of the cells' area compared to their area at normal osmolality.

Reversibility of the Hypo-Osmolar Changes in Membrane Properties

Figures 6 and 7 reveal severe changes in the passive electrical properties of the membrane under strongly hypo-osmotic conditions. The reversibility of these effects was investigated by use of the pretreatments given in the legend to Fig. 12. All media used in the shock and reversibility experiments were inositol media. It was found that after 30 min at low osmotic pressure (mean radius $a_{100} = 9.3 \pm 0.6$ μm) the cell radius returned to its original value on reverting to an isotonic medium ($a_{280(before)} = 7.0 \pm 0.2$ μm and $a_{280(after)} = 7.0 \pm 0.4$ μm). The decrease in C_m provoked by hypo-osmotic shock ($C_{m100} = 0.78 \pm 0.02$ μF/cm^2) also appears to be completely reversible ($C_{m280(before)} = 1.03 \pm 0.07$ μF/cm^2 and $C_{m280(after)} = 0.96 \pm 0.18$ μF/cm^2). On the other hand, the decrease in the apparent membrane conductivity after hypo-osmotic shock, ($G_{A280(before)} = 12.0 \pm 1.5$ mS/cm^2, $G_{A100} = 7.1 \pm 0.9$ mS/cm^2) was not fully reversible $G_{A280(after)} = 8.2 \pm 1.9$ mS/cm^2 ($P < 0.05$, *see* Fig. 12).

The ability of the cells to reversibly change their radius and capacity suggests that hypo-osmotic shock is not necessarily damaging to the cells. The change in G_A is of uncertain significance, not least because it is uncertain whether it results from a decrease in G_m or in K_S (or both).

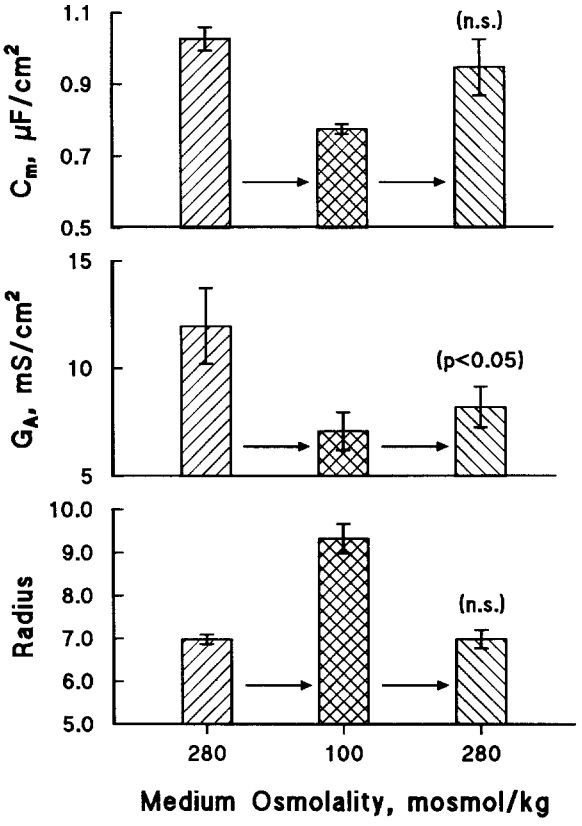

Fig. 12. The behavior of C_m, G_A and cell radius of G8 cells after hypo-osmotic shock and after return to normal osmolality. The G8 cells were washed three times either with inositol solution of osmolality 280 mOsm (columns labeled *280*) or 100 mOsm (labeled *100*). The righthand bar graphs (also labeled *280*) depict cells that were first washed twice at 100 mOsm, and after 30-min incubation were washed three times at 280 mOsm. The hypo-hyper-osmotic shock sequence caused differences significant at the levels indicated. *n.s.* indicates not highly significant ($P > 0.05$). The divergence of these data from those shown in Fig. 7 (especially in the case of the G_A values) may have been due to day-to-day fluctuations in membrane properties or to long-term change in the cell line after prolonged cultivation.

Discussion

Validity of the Rotation Theory

The use of Eq. (10) to derive parameters such as C_m and G_A from rotation data depends on several assumptions: that we are dealing with a thin, single, shell; that $\sigma_m \ll \sigma_o \ll \sigma_i$; and that the properties of the cell membrane do not change over the frequency range used.

The agreement of the experimental rotation spectra (Fig. 3 and Table) with the theoretical spectral function for a single-shelled particle justifies consideration of the cells as such objects. The highly linear dependence of $f_c \cdot a$ on σ_o (Figs. 4 and 5), and the consequent good fit to Eq. (10), is further justification of the single-membrane model, as well as substantiation of the assumptions required to derive an analytical expression for C_m and G_A. The internal membranes of the cell (especially the nuclear membrane) do not appear to have a significant influence on the results [24], presumably because the interior of the cell can be considered as an isopotential and because the nuclear membrane conductivity is high [11]. The good linearity of the plots in Figs. 4 and 5 also rules out the presence of significant dispersion in membrane properties, at least over the frequency range used (4–20 kHz). A dispersion would cause a decrease in C_m and an increase in G_m as the frequency is raised. Consideration of Eq. (10) shows that both of these would tend to give upwardly curved plots of $f_c \cdot a$ against σ. These are not observed (*see* Figs. 4 and 5): the worst-case correlation coefficient was 0.995: this corresponds to a maximum decrease in C_m over the frequency range of about 10% (G_m neglected).

In media of 280 mOsm, the fit of the mean spectra to theoretical is not quite as good as that at 150 mOsm or 75 mOsm (Table). Further, the rotation speed of the cells is only close to theoretical in extremely hypotonic media (Figs. 10 and 11). We believe that the cause of these deviations from some aspects of rotation theory to be the presence of microvilli on the membrane surface. As discussed below, these are only present at the higher osmolalities. When present, they cause the membrane to behave as a heterogeneous structure (which can only be *approximated* to a thin, uniform layer), and to increase the hydrodynamic resistance of the cell.

Volume and Capacitance Changes

Comparison between the SP2, and G8, and the L-cells reveals some interesting parallels between the physical and the electrical data.

The initial parts of the van't Hoff plots (Fig. 2) for SP2 and G8 cells are almost ideal, as if these cells can increase their membrane area very easily. By contrast, the L-cells seem to resist volume increase until the osmolality is reduced below 150 mOsm. Further dilution of the medium causes the cell volume to increase more rapidly, as if the L-cells possess a structure which yields at this point. Corresponding to the physical rigidity of these cells, the C_m value of the L-cells shows little hypo-osmotic effect until 150 mOsm, below which value it decreases rapidly.

In the case of SP2 and G8 cells (Fig. 2), reduction of the osmolality to below 150 mOsm causes less increase in cell volume than expected from an ideal osmometer. This may have been due to loss of cellular osmoticum, or to a decrease of the osmotic coefficient, both of which are expected after permeabilization of the membrane. The fact that the volume change was reversible (Fig. 12) indicates that the main effect was a change in osmotic coefficient.[3] Whatever the explanation, it is apparent that at 150 mOsm and below, the plasma membrane of SP2 and G8 cells begins to show signs of losing its nature as a physical barrier. Once again, the electrical measurements show an interesting parallel: there is a capacitance minimum at 185 mOsm (SP2) or 150 mOsm (G8).

These results become significant if the cause of the changes in C_m are considered. If the membrane were flat and of constant volume, the increase of membrane area which results from hypo-osmotic shock would be expected to cause a decrease in membrane thickness, and therefore an increase in C_m (*see* Eq. (8)). Clearly the membrane does not thin, because C_m decreases. On the other hand, electron micrographs show that microvilli become less evident after hypo-osmotic shock [28], and a link with the hypo-osmotically mediated decrease in C_m has been suggested before [11, 17].

If we interpret the C_c data (Eq. (13)) in terms of membrane area (only permissible if the microvilli are short or not radially directed, as for Eq. (9)), then the data for SP2 and G8 cells (Figs. 6*C* and 7*C*) suggest that the total membrane area ($X \cdot 4\pi a^2$) stays constant until the osmolality is decreased below about 200 mOsm. However, it increases rapidly below 150 mOsm.

Taken together, the volume, the C_m and the C_c data suggest the following:

(i) the apparently high C_m values of many animal cells [5, 17] are due to their possession of many microvilli: the true membrane capacity (C_{mu}) is considerably lower.

(ii) In response to moderate hypo-osmotic challenge, the microvilli provide an easily available reserve of membrane that enables the cell to behave as a perfect osmometer. (This applies to the SP2 and

[3] It can be argued that the nonideal osmotic behavior of the SP2 and G8 cells could also have been due to selective elimination of larger cells by severe hypo-osmotic shock (perhaps because of the lower ability of the large cells to increase their surface?). Even if the surviving "smaller" cells are ideal osmometers, this would cause an *apparent* violation of van't Hoff's law. Unfortunately for this hypothesis, the cells which were most badly affected by extreme hypo-osmolality (the L-cells) exhibited relatively large volumes at low osmolalities.

G8 cells; L-cells seem to have a structure that resists area expansion at moderate degrees of hypo-osmolality).

(iii) Once this membrane reserve has been used up, the cell surface becomes ideally spherical, and $C_m = C_{mu}$. Further surface area expansion cannot occur unless the thickness decreases (which does not occur to much extent, because C_m stays almost constant towards lower osmolalities), or else if "extra" membrane (not previously apparent at the surface) is made available. C_c almost doubles as the osmolality is decreased from 150–180 mOsm to 60 mOsm (Figs. 6*C* and 7*C*) so considerable quantities of membrane must be available from somewhere.

(iv) This "extra" membrane is only incorporated at the cost of some loss of membrane function. SP2 and G8 cells begin to show loss of membrane impermeability, while L-cells start to lyse. It can be speculated that the stretching forces begin to form pores in the membrane (as suggested by the G_A data, *see below*), and/or that the new membrane comes from some internal organelle, and is not as impermeable as normal plasma membrane.

(v) There is some evidence for a *slight* degree of membrane stretch. This is the small decrease in C_m as the osmolality was decreased to just below that which gave the minimum C_m (Figs. 6*A* and 7*A*). The relative increase in C_m (0.826/0.770 = 1.07 for SP2, and 0.827/0.771 = 1.07 for G8) corresponds (Eq. (8)) to a decrease in membrane thickness of 7%, assuming that the permittivity does not change. At constant membrane volume, this translates to a 7% stretch, which can be compared to the 6% stretch measured by electrical sizing of erythrocytes [30].

(vi) Reversal of the osmotic shock (Fig. 12) causes the cells to recover their original size and C_m, so that it appears as if the new membrane can be removed again, and that something resembling the original microvilli is re-formed. The fact that the G_A does not recover may mean that the changes to the glycocalix are not reversible.

Membrane Conductivity and Surface Conductance

The results on G_A, although exhibiting more scatter than those on C_m, do add some details to the above picture. The broad decrease in G_A of SP2 and of G8 cells as the osmolality is decreased from 280 mOsm to 150 or 180 mOsm, respectively, can be at least partly explained by a decrease in G_m. If we replace C_m and C_{mu} in Eq. (9) by G_m and G_{mu}, we should expect parallel behavior of G_m and C_m. In fact, the changes in G_A are greater than those in C_m, especially for G8 cells. It therefore appears that a significant part of the G_A is due to the K_S of these cells: even if K_S stays constant, this contribution will decrease as the cell radius decreases (*see* Eq. (2)). It is also likely that the K_S itself decreases as the cells expand (due to a reduction of glycocalix thickness, *see* Eq. (1), assuming constant volume).

Exposure of SP2 and G8 cells to extremely hypo-osmotic media (<150 mOsm) causes the G_A to increase again. It seems highly unlikely that K_S can increase as the cells swell (which would correspond to an increase of glycocalix thickness), so that it must be concluded that a large increase in G_m occurs. This corresponds to the increases in membrane permeability that could be deduced from the van't Hoff plots.

In contrast to the data on C_m, the osmotic shock reversal experiment (Fig. 12) showed that the decrease in G_A at 100 mOsm could not be restored. This indicates a permanent decrease in G_m or in K_S (it is not possible to say which).

The fact that pronase-treated G8 cells exhibit lower G_A than controls (Fig. 9) when measured at 280 mOsm (but not at 150 mOsm or 75 mOsm) indicates that the component of the G_A that is removed by pronase is the K_S, which is as expected if pronase removes the glycocalix.

Effects of Membrane-Protein Mobility

It has been pointed out [26] that the field-induced, lateral movement of proteins in biological membranes should give an increment to the membrane capacitance at low frequencies, with a dispersion in the kHz region (apparently close to 100 kHz in the case of bacterial protoplasts [23]). As stated above (*see* Validity of Rotation Theory) we see no evidence for significant dispersion (at most, a 10% change in C_m) in the animal cell lines in the frequency range (4–20 kHz) used here. Therefore, the decreases of 30%–70% in C_m seen with decreasing osmolality are very unlikely to have been due to changes in a protein-mobility dispersion. In addition, it seems reasonable to suppose that the protein mobility mechanism should give an increase, not the observed decrease, in C_m (measured at a given frequency) with decreasing osmolality. This is because the disruption of membrane structure, such as links with the cytoskeleton, should cause an increase in membrane-protein mobility. Therefore, it may at first sight seem possible that the small increase in C_m on the hypo-osmolar side of the C_m-minimum, *see* (v) above, may have been due to an increase in mobility and in the dispersion frequency. However, the fact that G_A increases concomitantly with C_m seems to rule this out, because conductivity and

permittivity move in opposite directions as a dispersion region is traversed [31].

Comparison with Literature Values

The values of the membrane capacity of SP2 myeloma ($1.01 \pm 0.04\ \mu F/cm^2$) and G8 ($1.09 \pm 0.03\ \mu F/cm^2$) cells in isotonic conditions (280 mosmol/kg) reported here are in good agreement with values accepted as typical for biological membranes [31], and more specifically with those obtained [12] on mouse myeloma (P3X63Ag8) cells by means of either the micropipette technique ($C_m = 1.03 \pm 0.09\ \mu F/cm^2$) or of impedance analysis of suspensions ($0.87\ \mu F/cm^2$). They are also close to the $1.4\ \mu F/cm^2$ obtained by the electrorotation of DS19 erythroleukaemic cells [32], and to the earlier results on SP2 cells ($C_m = 1.16 \pm 0.03\ \mu F/cm^2$ [9]).

On the other hand, the micropipette technique [12] gives much lower values (90–100 $\mu S/cm^2$) for G_m for mouse myeloma cells in isotonic conditions, some 100-fold lower than the G_A values obtained for SP2 and G8 cells in this work. The discrepancy may be due to the K_S contribution to G_A (K_S does not affect micropipette measurements), as indeed suggested by the observation that pronase treatment reduced the K_S to close to zero. However, the possible existence of a dispersion below the range of frequencies used for rotation would also raise the G_A (*see* [5, 9]).

The C_m data on isotonic L-cells ($2.18 \pm 0.10\ \mu F/cm^2$) are somewhat higher than the usual range for biomembranes [31]. However, this is normal for fibroblasts: $C_m = 1.52 \pm 0.26\ \mu F/cm^2$ was obtained on rabbit fibroblasts by feedback-controlled levitation [25]. The high C_m value of L-cells compared to SP2 or G8 cells presumably reflects a much higher degree of membrane folding in the L-cells. This is expected, because in their native (surface-attached) state, fibroblasts have a highly flattened form. The fact that L-cells, despite their large excess of membrane, resist expansion in response to moderate hypo-tonicities is presumably a consequence of cytoskeletal structure.

Conclusion

The mechanisms of expansion of the apparent area of cultured myeloma and hybridoma cells during hypo-osmotic shock have been elucidated. The capacitance and rotation speed data confirm electron-microscope images that show a progressive disappearance of the surface microvilli as the cell radius increases [12, 28]. This may be the only mechanism operating for mild osmotic shifts (from 280 mOsm to about 200 mOsm), because the total area seems to stay constant in this range.

More severe osmotic shifts cause, besides loss of the remaining microvilli, a progressive increase of the accessible membrane area (it can almost double). This is presumably by utilization of internal or stored membrane. These mechanisms seem also to apply to fibroblasts (L-cells), although these respond only to more extreme hypo-osmotic stress.

The observation of a slight increase in membrane capacitance of the myeloma and hybridoma cells as the tonicity is reduced through the 60–50% range indicates that membrane stretch seems also to occur, but only to the extent of about 7%.

The results raise interesting questions as to the origin of the membrane that is effectively instantly available, as well as to the mechanism involved in its deployment, which appears to be largely reversible.

We thank Mr. B.G. Klarmann for his help with the measurements. This work was supported by grants of the DFG (SFB 176 B5 to U.Z. and W.M.A.) and of the BMFT (DARA 50 WB 9212 to U.Z.). We also thank the Umweltbundesamt, Berlin, for support enabling the construction of some of the rotation generators used in this work.

References

1. Ahkong, Q.F., Lucy, J.A. 1986. Osmotic forces in artificially induced cell fusion. *Biochim. Biophys. Acta* **858:**206–216
2. Arnold, W.M. 1988. Analysis of optimum electro-rotation technique. *Ferroelectrics* **86:**225–244
3. Arnold, W.M., Gessner, A.G., Zimmermann, U. 1993. Dielectric measurements on electromanipulation media. *Biochim. Biophys. Acta* **1157:** (*in press*)
4. Arnold, W.M., Klarmann, B.G., Sukhorukov, V.L., Zimmermann, U. 1992. Membrane accommodation in hypo-osmotically-treated, and giant electrofused cells. *Biochem. Soc. (Lond.) Transactions* **20:**120S
5. Arnold, W.M., Schmutzler, R.K., Al-Hasani, S., Krebs, D., Zimmermann, U. 1989. Differences in membrane properties between unfertilised and fertilised single rabbit oocytes demonstrated by electro-rotation. Comparison with cells from early embryos. *Biochim. Biophys. Acta* **979:**142–146
6. Arnold, W.M., Schwan, H.P., Zimmermann, U. 1987. Surface conductance and other properties of latex particles measured by electrorotation. *J. Phys. Chem.* **91:**5093–5098
7. Arnold, W.M., Zimmermann, U. 1982. Rotation of an isolated cell in a rotating electric field. *Naturwissenschaften* **69:**297
8. Arnold, W.M., Zimmermann, U. 1983. Patent application, official designation P3325 843.0, received at the Patent Office, FRG, July 18, 1983
9. Arnold, W.M., Zimmermann, U. 1988. Electro-rotation: development of a technique for dielectric measurements on individual cells and particles. *J. Electrostatics* **21:**151–191
10. Arnold, W.M., Zimmermann, U. 1989. Measurements of dielectric properties of single cells or other particles using direct

observation of electro-rotation. *In:* Proceedings of The First International Conference on Low Cost Experiments in Biophysics, Cairo, 18–20 December, 1989. pp. 1–13
11. Asami, K., Takahashi, Y., Takashima, S. 1989. Dielectric properties of mouse lymphocytes and erythrocytes. *Biochim. Biophys. Acta* **1010**:49–55
12. Asami, K., Takahashi, Y., Takashima, S. 1990. Frequency domain analysis of membrane capacitance of cultured cells (HeLa and myeloma) using the micropipette technique. *Biophys. J.* **58**:143–148
13. Chizmadzhev, Yu.A., Kuzmin, P.I., Pastushenko, V.Ph. 1985. Theory of the dielectrophoresis of vesicles and cells. *Biologicheskie Membrany* **2**:1147–1161 (*in Russian*)
14. CRC 1988. *CRC Handbook of Chemistry and Physics*, R.C. Weast, editor. CRC Press, Boca Raton, FL
15. Earle, W.R. 1943. Production of malignancy in vitro. IV. The mouse fibroblast cultures and changes seen in the living cells. *J. Nat. Cancer Inst.* **4**:165–212
16. Foung, S., Perkins, S., Kafadar, K., Gessner, P., Zimmermann, U. 1990. Development of microfusion techniques to generate human hybridomas. *J. Immunol. Meth.* **134**:35–42
17. Freitag, R., Schügerl, K., Arnold, W.M., Zimmermann, U. 1989. The effect of osmotic and mechanical stresses and enzymatic digestion on the electro-rotation of insect cells (*Spodoptera frugiperda*). *J. Biotechnol.* **11**:325–336
18. Fuhr, G., Arnold, W.M., Hagedorn, R., Müller, T., Benecke, W., Wagner, B., Zimmermann, U. 1992. Levitation, holding, and rotation of cells within traps made by high frequency fields. *Biochim. Biophys. Acta* **1108**:215–223
19. Fuhr, G., Glaser, R., Hagedorn, R. 1986. Rotation of dielectrics in a rotating electric high-frequency field. *Biophys. J.* **69**:395–402
20. Fuhr, G., Hagedorn, R. 1988. Grundlagen der Elektrorotation. *In:* Colloquia Pflanzenphysiologie. H. Göring und P. Hoffmann, editors, Nr. 11. Humboldt-Universität zu Berlin, Berlin
21. Fuhr, G., Kuzmin, P.I. 1986. Behavior of cells in rotating electric fields with account to surface charges and cell structures. *Biophys. J.* **50**:789–795
22. Glaser, R., Fuhr, G., Gimsa, J. 1983. Rotation of erythrocytes, plant cells, and protoplasts in an outside rotating electric field. *Studia Biophysica* **96**:11–20
23. Harris, C.M., Kell, D.B. 1985. On the dielectrically observable consequences of the diffusional motions of lipids and proteins in membranes. 2. Experiments with microbial cells, protoplasts and membrane vesicles. *Eur. Biophys. J.* **13**:11–24
24. Hu, X., Arnold, W.M., Zimmermann, U. 1990. Alterations in the electrical properties of T and B lymphocyte membranes induced by mitogenic stimulation. Activation monitored by electro-rotation of single cells. *Biochim. Biophys. Acta* **1021**:191–200
25. Kaler, K.V.I.S., Jones, T.B. 1990. Dielectrophoretic spectra of single cells determined by feedback controlled levitation. *Biophys. J.* **57**:173–182
26. Kell, D.B., Harris, C.M. 1985. On the dielectrically observable consequences of the diffusional motions of lipids and proteins in membranes. 1. Theory and overview. *Eur. Biophys. J.* **12**:181–197
27. Klöck, G., Zimmermann, U. 1990. Facilitated electrofusion of vacuolated × evacuolated oat mesophyll protoplasts in hypo-osmotic media after alignment with an alternating field of modulated strength. *Biochim. Biophys. Acta* **1025**:87–93
28. Knutton, S., Jackson, D., Graham, J.M., Micklem, K.J., Pasternak, C.A. 1976. Microvilli and cell swelling. *Nature* **262**:52–54
29. Lamb, H. 1906. Hydrodynamics, 3rd edn., Article 322. Cambridge University, Cambridge, UK
30. Mela, M., Eskelinen, S. 1984. Normal and homogeneous red blood cell populations over a wide range of hyper-iso-hypotonic media. III. Corrected volumes in Coulter Counter measurements. *Acta Physiol. Scand.* **122**:515–525
31. Pethig, R. 1979. Dielectric and Electronic Properties of Biological Materials. John Wiley and Sons, Chichester
32. Pethig, R. 1991. Application of A.C. electrical fields to the manipulation and characterisation of cells. *In:* Automation in Biotechnology. I. Karube, editor. pp. 159–185. Elsevier Science Publishers B.V.
33. Sauer, F.A., Schlögl, R.W. 1985. Torques exerted on cylinders and spheres by external electromagnetic fields. A contribution to the theory of induced cell rotation, *In:* Interaction Between Electromagnetic Fields and Cells. A. Chiabrera, C. Nicolini and H.P. Schwan, editors. pp. 203–251. Plenum, New York
34. Schmitt, J.J., Zimmermann, U. 1989. Enhanced hybridoma production by electrofusion in strongly hypo-osmolar solutions. *Biochim. Biophys. Acta* **983**:42–50
35. Schwan, H.P. 1985. Dielectric properties of the cell surface and electric field effects on cells. *Studia Biophysica* **110**:13–18
36. Schwan, H.P. 1988. Dielectric spectroscopy and electro-rotation of biological cells. *Ferroelectrics* **86**:205–223
37. Schwan, H.P. 1989. Dielectrophoresis and rotation of cells. *In:* Electroporation and Electrofusion in Cell Biology. E. Neuman, A.E. Sowers and C.A. Jordan, editors. pp. 3–21. Plenum, New York
38. Shulman, M., Wilde, C.D., Köhler, G. 1978. A better cell line for marking hybridomas secreting specific antibodies. *Nature* **276**:269–270
39. Steponkus, P.L., Lynch, D.V. 1989. Freeze/thaw-induced destabilization of the plasma membrane and the effects of cold acclimation. *J. Bioenerg. Biomembr.* **21**:21–41
40. Zimmermann, U., Arnold, W.M. 1983. The interpretation and use of the rotation of biological cells. *In:* Coherent Excitations in Biological Systems. H. Fröhlich and F. Kremer, editors. pp. 211–221. Springer-Verlag, Berlin
41. Zimmermann, U., Gessner, P., Schnettler, R., Perkins, S., Foung, S.K.H. 1990. Efficient hybridization of mouse-human cell lines by means of hypo-osmolar electrofusion. *J. Immunol. Meth.* **134**:43–50

Received 13 May 1992; revised 4 August 1992